DYNAMIC EARTH PRESSURES ON BASEMENT WALL

by

Hiroshi Tajimi

SYNOPSIS

The present paper describes a theoretical analysis of earth pressures on basement walls on a basis of the two-dimensional wave propagation theory. The walls are assumed to undergo periodic vibrations of horizontal translation and rocking. The results are given for the distributions of earth pressure on the wall and the coefficients of soil reaction, which are expressed by real and imaginary components varying with frequency. Furthermore, the theoretical predictions were examined by field experiments of moderate scale.

INTRODUCTION

Previously[1], the writer presented the dynamic analysis of a cylindrical structure embedded in elastic soil. The present paper is an extension and concerns a detailed analysis of earth pressure acting on basement walls. In particular, it interests in the evaluation of radiation damping associated with the walls.

The theory of footings resting on elastic half-space is fundamental to investigate the problem of soil-structure interaction. As similar, the theory of walls embedded in elastic medium will be considered to be important to the earthquake response of a building having basement. The subsequent analysis is based on the theory of two-dimensional wave propagation in a homogeneous elastic body. Mathematical model is made as shown in Fig. 1. It consists of a quarter-infinite field, whose vertical boundary is imposed by lateral deformation accompanied by the movement of the basement wall.

THEORETICAL ANALYSIS ON THE CASE OF HORIZONTAL TRANSLATION OF THE WALL

As shown in Fig. 1, the origin of coordinates is put on the top of the wall, with the x-axis along the free surface and the z-axis vertically downward. The analysis is divided into two steps. The first step is the application of the image method to the domain $0 < z$. It requires the condition that the boundary displacement imposed by the movement of the wall is to be given symmetry with respect to the x-axis. Then, the resulting stress pattern will become symmetry about the x-axis. Successively, the second step is to eliminate the normal stress which was generated at the boundary $z = 0$ as a result of the first step analysis, because the plane $z = 0$ should be originally a free surface. Thus, two sets of potentials (φ_1, Ψ_1) and (φ_2, Ψ_2) are introduced as particular solutions of the two-dimensional wave equations, corresponding to the two steps of analysis.

Professor, College of Science and Engineering, Nihon University

As well known[2], the displacements denoted by u and w in the x- and z-direction, respectively, are derived from

$$u_s = \frac{\partial \varphi_s}{\partial x} + \frac{\partial \Psi_s}{\partial z}, \qquad w_s = \frac{\partial \varphi_s}{\partial z} - \frac{\partial \Psi_s}{\partial x}, \qquad s = 1, 2 \tag{1}$$

where the subscripts 1 and 2 are referred to the number of the step of analysis. The first set of potentials (φ_1, Ψ_1) have the form

$$\varphi_1 = \int_0^\infty A e^{-\alpha x} \cos pz \, dp, \qquad \Psi_1 = \int_0^\infty B e^{-\beta x} \sin pz \, dp \tag{2}$$

which satisfy the symmetry condition of stresses and displacements with respect to the x-axis. A and B are functions of the parameter p. Besides, when the velocities of dilatational wave and shear wave are denoted by V_p and V_s, respectively, the following symbols are used:

$$\alpha^2 = p^2 - \ell^2, \qquad \beta^2 = p^2 - j^2, \qquad \ell = \omega / V_p, \qquad j = \omega / V_s$$

where α and β must be taken as positive real or positive imaginary in order to agree with the condition of waves decaying out or proceeding toward $|x| \to \infty$. When the height of wall is denoted by H, the boundary conditions are given by

$$\begin{aligned} u_1|_{x=0} &= U_0 e^{i\omega t} \qquad |z| < H \\ &= 0 \qquad\qquad |z| > H \end{aligned} \tag{3}$$

$$_1\tau_{xz}| = 0 \tag{4}$$

Eq. (3) can be expressed by the Fourier integral in the form

$$u_1|_{x=0} = U_0 e^{i\omega t} \frac{2}{\pi} \int_0^\infty \frac{\sin pH}{p} \cos pz \, dp \tag{5}$$

Substituting Eq. (2) into Eq. (1), one has

$$u_1 = \int_0^\infty (-\alpha A e^{-\alpha x} + p B e^{-\beta x}) \cos pz \, dp \tag{6}$$

Since Eq. (6) must be coincident with Eq. (5) at x = 0, one gets

$$-\alpha A + p B = \frac{2}{\pi} \frac{\sin pH}{p} U_0 e^{i\omega t} \tag{7}$$

The shearing stress at x = 0 is expressed by

$$\frac{_1\tau_{zx}}{G}|_{x=0} = \left(2 \frac{\partial^2 \varphi_1}{\partial x \partial z} - j^2 \Psi_1 - 2 \frac{\partial^2 \Psi_1}{\partial x^2}\right)_{x=0}$$

$$= \int_0^\infty [2A\alpha p - B(j^2 + 2\beta^2)] \sin pz \, dp$$

where G denotes the shearing modulus of soil. From the boundary condition of Eq. (4)

$$2A\alpha p - B(j^2 + 2\beta^2) = 0 \tag{8}$$

Solving Eqs. (7) and (8) for A and B, one obtains

$$A = \frac{2}{\pi} \frac{\sin pH}{p} \frac{2p^2 - j^2}{\alpha j^2} U_0 e^{i\omega t}, \qquad B = \frac{2}{\pi} \frac{\sin pH}{p} \frac{2p}{j^2} U_0 e^{i\omega t} \tag{9}$$

The normal stress $_1\sigma_z$ in the first step analysis can be written in the form

$$\frac{{}_1\sigma_z}{G} = -j^2\varphi_1 - 2\frac{\partial^2\varphi_1}{\partial x^2} - 2\frac{\partial^2\psi_1}{\partial x\,\partial z}$$

$$= \int_0^\infty [-(2\alpha^2 + j^2)\,Ae^{-\alpha x} + 2\beta p\,Be^{-\beta x}]\cos pz\,dp$$

Hence, the normal stress acting on the symmetry plane $z = 0$ will be easily obtained.

In the second step of analysis, the normal stress $\sigma_z|_{z=0}$ must vanish for satisfying the originally given conditions. For this purpose, the image method was employed again by constructing the symmetry image of the stress field with respect to the z-axis. Therefore, one considers

$$\frac{{}_1\sigma_z}{G}\Big|_{z=0} = \int_0^\infty [-(2\alpha^2 + j^2)\,Ae^{-\alpha|x|} + 2\beta p\,Be^{-\beta|x|}]\,dp \tag{10}$$

The Fourier transform of Eq. (10) defined by

$$\frac{{}_1\sigma_z}{G}\Big|_{z=0} = \int_{-\infty}^\infty L(q)\,e^{-ixq}\,dq \tag{11}$$

is given by

$$L(q) = \frac{1}{2\pi}\int_{-\infty}^\infty e^{ixq}\,dx \int_0^\infty [-(2\alpha^2 + j^2)\,Ae^{-\alpha|x|} + 2\beta p\,Be^{-\beta|x|}]\,dp \tag{12}$$

The integral included in the above equation can be evaluated as

$$\int_{-\infty}^\infty e^{-\alpha|x|}\,e^{ixq}\,dx = \lim_{\varepsilon\to+0}\int_{-\infty}^\infty e^{-(\alpha+\varepsilon)|x|}\,e^{ixq}\,dx$$

$$= \lim_{\varepsilon\to+0}\frac{2(\alpha+\varepsilon)}{(\alpha+\varepsilon)^2 + q^2}$$

Thus, substitution of A and B in Eq. (9) into Eq. (12) yields

$$L(q) = U_0\,e^{i\omega t}\frac{2}{\pi^2}\lim_{\delta\to0}\int_{0+i\delta}^{\infty+i\delta}\left[-\frac{2\alpha^2 + j^2}{q^2+\alpha^2}\,\frac{2p^2 - j^2}{j^2} + \frac{4\beta^2\,p^2}{q^2+\beta^2}\,\frac{1}{j^2}\right]\frac{\sin pH}{p}\,dp \tag{13}$$

Making use of the dimesionless symbols,

$$\frac{p}{j} = \zeta, \quad \frac{q}{j} = \xi, \quad \frac{V_s}{V_p} = \sqrt{\frac{1-2\nu}{2(1-\nu)}} = \gamma, \quad \frac{\omega H}{V_s} = \Omega \tag{14}$$

Eq. (13) can be written in the form

$$L(\xi) = U_0\,e^{i\omega t}\frac{2}{\pi^2}\lim_{\delta\to0}\int_{0+i\delta}^{\infty+i\delta}\left[\frac{-(2\zeta^2 - 2\gamma^2 + 1)(2\zeta^2 - 1)}{\zeta^2 + \xi^2 - \gamma^2} + \frac{4\zeta^4 - 4\zeta^2}{\zeta^2 + \xi^2 - 1}\right]\frac{\sin\zeta\Omega}{\zeta}\,d\zeta$$

$$= U_0\,e^{i\omega t}\frac{2}{\pi^2}\lim_{\delta\to0}\int_{0+i\delta}^{\infty+i\delta}\left[\frac{-(2\xi^2 - 2\gamma^2 + 1)(2\xi^2 - 1)}{\zeta^2 + \xi^2 - \gamma^2} + \frac{4\xi^4 - 4\xi^2}{\zeta^2 + \xi^2 - 1}\right]\frac{\sin\zeta\Omega}{\zeta}\,d\zeta \tag{15}$$

This integral can be solved by use of the formulae:

$$\lim_{\delta\to0}\int_{0+i\delta}^{\infty+i\delta}\frac{1}{\zeta^2 + \xi^2 - \gamma^2}\frac{\sin\zeta\Omega}{\zeta}\,d\zeta = \begin{cases} \dfrac{\pi}{2}\dfrac{1}{\xi^2 - \gamma^2}\left(1 - e^{-i\Omega\sqrt{\gamma^2 - \xi^2}}\right), & |\xi| < \gamma \\ \dfrac{\pi}{2}\dfrac{1}{\xi^2 - \gamma^2}\left(1 - e^{-\Omega\sqrt{\xi^2 - \gamma^2}}\right), & |\xi| > \gamma \end{cases} \tag{16}$$

$$\lim_{\delta\to 0}\int_{0+i\delta}^{\infty+i\delta}\frac{1}{\zeta^2+\xi^2-\gamma^2}\,\frac{\sin\zeta\Omega}{\zeta}\,d\zeta=\begin{cases}\dfrac{\pi}{2}\,\dfrac{1}{\xi^2-1}\,(1-e^{-i\Omega\sqrt{1-\xi^2}}), & |\xi|<1\\[2ex] \dfrac{\pi}{2}\,\dfrac{1}{\xi^2-1}\,(1-e^{-\Omega\sqrt{\xi^2-1}}), & |\xi|>1\end{cases}\tag{17}$$

As a consequence, the Fourier transform of ${}_1\sigma_z|_{z=o}$ is obtained as

$$L(\xi)=U_0\,e^{i\omega t}\,\frac{1}{\pi}\left[4\xi^2\{F_2(\xi)-F_1(\xi)\}+\frac{1-2\gamma^2}{\xi^2-\gamma^2}\,F_1(\xi)\right]\tag{18}$$

$$F_1(\xi)=\begin{cases}1-e^{-i\Omega\sqrt{\gamma^2-\xi^2}}, & |\xi|<\gamma;\\ 1-e^{-\Omega\sqrt{\xi^2-\gamma^2}}, & |\xi|>\gamma;\end{cases}\qquad F_2(\xi)=\begin{cases}1-e^{-i\Omega\sqrt{1-\xi^2}}, & |\xi|<1\\ 1-e^{-\Omega\sqrt{\xi^2-1}}, & |\xi|>1\end{cases}$$

For the second step of analysis, consider another set of potentials,

$$\varphi_2=\int_0^\infty Ce^{-\bar\alpha z}\cos qx\,dq,\quad \Psi_2=\int_0^\infty De^{-\bar\beta z}\sin qx\,dq,\tag{19}$$

$$\bar\alpha^2=q^2-\ell^2,\quad \bar\beta^2=q^2-j^2$$

These functions satisfy the boundary conditions $u|_{x=o}=0$ and $\tau_{xz}|_{x=o}=0$. The stresses are expressed by

$$\frac{{}_2\sigma_z}{G}=\int_0^\infty\left[(2q^2-j^2)\,Ce^{-\bar\alpha z}+2q\bar\beta\,De^{-\bar\beta z}\right]\cos qx\,dq$$

$$\frac{{}_2\tau_{xz}}{G}=\int_0^\infty\left[2q\sqrt{q^2-\ell^2}\,Ce^{-\bar\alpha z}+(2q^2-j^2)\,De^{-\bar\beta z}\right]\sin qx\,dq$$

Since the plane z = 0 is a free surface, it needs that

$$\sigma_z|_{z=0}=\sum_{s=1}^{2}{}_s\sigma_z|_{z=0}=0,\quad \tau_{xz}|_{z=0}=\sum_{s=1}^{2}{}_s\tau_{xz}|_{z=0}=0,\tag{20}$$

From ${}_1\tau_{xz}|_{z=o}=0$, one has

$${}_2\tau_{xz}|_{z=0}=0$$

In addition, instead of Eq. (11), one uses

$$\frac{{}_1\sigma_z}{G}|_{z=0}=2\int_0^\infty L(q)\cos qx\,dq$$

because L(q) is an even function. Thus,

$$(2q^2-j^2)\,C+2q\sqrt{q^2-j^2}\,D=-2L(q),\quad 2q\sqrt{q^2-\ell^2}\,C+(2q^2-j^2)\,D=0$$

These equations determine the unknowns C and D:

$$C=-\frac{2q^2-j^2}{F(q)}\,2L(q),\quad D=\frac{2q\sqrt{q^2-\ell^2}}{F(q)}\,2L(q)$$
$$F(q)=(2q^2-j^2)^2-4q^2\sqrt{q^2-\ell^2}\,\sqrt{q^2-j^2}\tag{21}$$

The earth pressure acting on the basement wall is given by

$$-\frac{\sigma_x}{G}|_{x=0}=-\frac{{}_1\sigma_x}{G}|_{x=0}-\frac{{}_2\sigma_x}{G}|_{x=0}=\sum_{s=1}^{2}\left(j^2\varphi_s+2\frac{\partial^2\varphi_s}{\partial z^2}-2\frac{\partial^2\Psi_s}{\partial x\,\partial z}\right)_{x=0}$$

$$=-\int_0^\infty(2p^2-j^2)\,A\cos pz\,dp+\int_0^\infty 2\beta\,pB\cos pz\,dp+$$

$$= -\int_0^\infty (2p^2 - j^2)\, A \cos pz\, dp + \int_0^\infty 2\beta\, pB \cos pz\, dp \tag{22}$$

Substituting the functions A, B, C and D from Eqs. (9) and (21) into the above equation and rewriting it in the dimensionless form by use of the notations defined in Eq. (14), one obtains

$$-\frac{{}_1\sigma_x}{G}\Big|_{x=0} = -U_0\, e^{i\omega t}\, \frac{2}{\pi}\, \frac{\Omega}{H} \lim_{\delta\to 0} \int_{0+i\delta}^{\infty+i\delta} \frac{(2\zeta^2-1)^2 - 4\zeta^2\sqrt{\zeta^2-\gamma^2}\,\sqrt{\zeta^2-1^2}}{\sqrt{\zeta^2-\gamma^2}} \times \frac{\sin \zeta\Omega}{\zeta} \cos\left(\zeta\Omega \frac{z}{H}\right) d\zeta \tag{23}$$

$$-\frac{{}_2\sigma_x}{G}\Big|_{x=0} = -U_0\, e^{i\omega t}\, \frac{2}{\pi}\, \frac{\Omega}{H} \lim_{\delta\to 0} \int_{0+i\delta}^{\infty+i\delta} \left[4\xi^2 \{ F_2(\xi) - F_1(\xi) \} + \frac{1-2\gamma^2}{\xi^2-\gamma^2} F_1(\xi) \right] \times \frac{(2\xi^2-2\gamma^2+1)(2\xi^2-1)\, e^{-\sqrt{\xi^2-\gamma^2}\,\Omega z/H} - 4\xi^2\sqrt{\xi^2-\gamma^2}\,\sqrt{\xi^2-1}\, e^{-\sqrt{\xi^2-1}\,\Omega z/H}}{(2\xi^2-1)^2 - 4\xi^2\sqrt{\xi^2-\gamma^2}\,\sqrt{\xi^2-1}} d\xi \tag{24}$$

In particular, the case of static movement of the wall is obtained by $\omega \to 0$, namely, ℓ, $j \to 0$:

$$\lim_{\omega\to 0} -\frac{{}_1\sigma_x + {}_2\sigma_x}{G}\Big|_{x=0} = -U_0\, \frac{8}{\pi}\, \frac{H^2}{1-\nu}\, \frac{z}{(z-H)(z+H)^3} \tag{25}$$

This equation agrees with that already obtained by W. D. Liam Finn[3].

The integral of Eq. (23) can be obtained by the analytical method of separating the integration domain into the three ranges, $0 < \xi < \gamma$, $\gamma < \xi < 1$, $1 < \xi < \infty$, and expanding the integrands by the power series in each domain. Thus, the integrals become possible by use of the trigonometric substitution. The denominator of the integrand of Eq. (24) is known as the Rayleigh function which has the pole ξ_R and two branch points γ and 1 on the real axis. The contour of integration is shown in Fig. 2. The numerical results of total pressure distribution are graphically plotted in Fig. 3 for the dimensionless functions $S_1(\omega, z)$ and $S_2(\omega, z)$ which are defined by

$$-\sigma_x|_{x=0} = \frac{G}{H} U_0\, e^{i\omega t} [\, S_1(\omega, z) + i\, S_2(\omega, z)\,] \tag{26}$$

The dimensionless frequency H/V_S is used as a parameter. Furthermore, the distributions depend on the Poisson's ratio. Here, the velocity ratio γ is specified as 1/2 and 1/3, which correspond to the Poisson's ratios $\upsilon = 0.3333$ and 0.4375, respectively. As found in the figure, the real part $S_1(\omega, z)$ has a singular point at the depth $z = H$ owing to discontinuity of the boundary displacement, while the imaginary part $S_2(\omega, z)$ varies little along the depth. The resultant force acting the basement wall can be determined from

$$-\int_0^H \sigma_x|_{x=0}\, dz = GU_0\, e^{i\omega t} [\, K_1(\omega) + i K_2(\omega)\,] \tag{27}$$

where $G[K_1(\omega) + iK_2(\omega)]$ is the complex form of modulus of soil reaction. In the numerical integration of Eq. (27), one must avoid the singular point. From the practical point of view, it was assumed that the stress in the range of $z > 0.8H$ holds the value at the depth $z = 0.8H$. Plots

shown in Fig. 4 indicate thus obtained relationships of the complex modulus $K_1 + iK_2$ to the dimensionless frequency $\omega H/V_s$.

As a simple model, consider a soil rod having cross-sectional area H x 1 and extending laterally toward the positive x-direction. When the wall displacement $U_o \exp i\omega t$ is applied at x = 0, the end compressional stress can be written as

$$-\sigma_x|_{x=0} = U_0 e^{i\omega t} \frac{i\omega}{V_p} E$$

$$= \frac{G}{H} U_0 e^{i\omega t} \; i \frac{\omega H}{V_s} \frac{V_s}{V_p} 2(1+\nu) \tag{28}$$

This equation corresponds to Eq. (26). It follows that the function K_2 is approximated by

$$K_2 = \frac{\omega H}{V_s} \frac{V_s}{V_p} 2(1+\nu) \tag{29}$$

For the specified values of γ, one has

$$K_2 = \frac{\omega H}{V_s} 1.333, \quad \text{for} \quad r = 1/2\,; \qquad K_2 = \frac{\omega H}{V_s} 0.958, \quad \text{for} \quad r = 1/3$$

It is interesting that this simple relation agrees fairly with the rigorous relation shown in Fig. 4.

THEORETICAL ANALYSIS ON THE CASE OF ROCKING OF THE WALL

The analysis can be proceeded in the same way with the case of horizontal translation of the wall. If the displacement at the top of the wall is denoted by $U_o \exp i\omega t$, the boundary conditions are given by

$$u|_{x=0} = U_0 (1 - z/H) e^{i\omega t}, \quad |z| < H\,; \qquad \tau_{xz}|_{x=0} = 0$$
$$= 0, \quad |z| > H\,; \tag{30}$$

The, the functions A and B corresponding to Eq. (9) are obtained as

$$A = -\frac{2}{\pi H} \frac{1-\cos pH}{p^2} \frac{2p^2 - j^2}{\alpha j^2} U_0 e^{i\omega t}, \qquad B = -\frac{2}{\pi H} \frac{1-\cos pH}{p^2} \frac{2p}{j^2} U_0 e^{i\omega t} \tag{31}$$

Successively, the function corresponding to Eq. (18) is expressed by

$$L(\xi) = U_0 e^{i\omega t} \frac{1}{\pi \Omega} \left[4\xi^2 \{ F_4(\xi) - F_3(\xi) \} - \frac{1-2r^2}{\xi^2 - r^2} F_3(\xi) \right] \tag{32}$$

$$F_3(\xi) = \begin{cases} \Omega + i \dfrac{1 - e^{-i\Omega\sqrt{r^2-\xi^2}}}{\sqrt{r^2-\xi^2}}, & |\xi| < r\,; \\ \Omega - \dfrac{1 - e^{-\Omega\sqrt{\xi^2-r^2}}}{\sqrt{\xi^2-r^2}}, & |\xi| > r\,; \end{cases} \qquad F_4(\xi) = \begin{cases} \Omega + i \dfrac{1 - e^{-i\Omega\sqrt{1-\xi^2}}}{\sqrt{1-\xi^2}}, & |\xi| < 1 \\ \Omega - \dfrac{1 - e^{-\Omega\sqrt{\xi^2-1}}}{\sqrt{\xi^2-1}} & |\xi| > 1 \end{cases}$$

Thus, the earth pressure is given by the integrals

$$-\frac{\sigma_x}{G}|_{x=0} = -\frac{U_0}{H} e^{i\omega t} \frac{2}{\pi} \lim_{\delta \to 0} \int_{0+i\delta}^{\infty+i\delta} \frac{(2\zeta^2-1)^2 - 4\zeta^2\sqrt{\zeta^2-r^2}\sqrt{\zeta^2-1}}{\sqrt{\zeta^2-r^2}}$$

$$\times \frac{1-\cos\zeta\Omega}{\zeta^2} \cos\left(\zeta\Omega \frac{z}{H}\right) d\zeta \tag{33}$$

$$-\frac{{}_2\sigma_x}{G}\Big|_{x=0} = -\frac{U_0}{H} e^{i\omega t} \frac{2}{\pi} \lim_{\delta\to 0} \int_{0+i\delta}^{\infty+i\delta} \left[4\xi^2 \{ F_4(\xi) - F_3(\xi) \} + \frac{1-2r^2}{\xi^2-r^2} F_3(\xi) \right]$$

$$\times \frac{(2\xi^2-2r^2+1)\, e^{-\sqrt{\xi^2-r^2}\,\Omega z/H} - 4\xi^2 \sqrt{\xi^2-r^2}\,\sqrt{\xi^2-1}\, e^{-\sqrt{\xi^2-1}\,\Omega z/H}}{(2\xi^2-1)^2 - 4\xi^2 \sqrt{\xi^2-r^2}\,\sqrt{\xi^2-1}} \, d\xi$$

The numerical results of earth pressure are plotted in Fig. 5 for the dimensionless stress distributions $R_1(\omega, z)$ and $R_2(\omega, z)$ which are defined by

$$-\sigma_x|_{x=0} = -({}_1\sigma_x + {}_2\sigma_x)|_{x=0} = \frac{G}{H} U_0 e^{i\omega t} [R_1(\omega, z) + i R_2(\omega, z)] \tag{34}$$

It is noted in this figure that the real part $R_1(\omega, z)$ vanishes at a depth of about 0.7H and reverses sign below this. It causes from the concentrated force to be applied at the bottom not so as to be moved. The imaginary part is characterized by being distributed uniformly as same as the case of the horizontal translation, although the magnitude is rather smaller. The resultant moment about the bottom is determined from

$$-\int_0^H (H-z)\, \sigma_x|_{x=0}\, dz = GU_0 He^{i\omega t} [M_1(\omega) + i M_2(\omega)] \tag{35}$$

Plots shown in Fig. 6 indicate the complex modulus $M_1 + iM_2$.

COMPARISON OF THE PRESENT THEORY AND EXPERIMENTS

The field test to be compared to the present theory was performed by S. Niwa[4]. He measured oscillating earth pressures acting on the back of a test retaining wall of gravity type. This test wall was made by concrete with 3 m high, 0.6 m wide at the top, 1.5 m wide at the bottom and 5 m in length. It was placed on the bottom of a trench which was excavated in loam soil up to the 3 m depth. The trench had a slope on the side facing the back of the test wall, which was backfilled by sand. To excite the horizontal translation of the wall, the sinusoidal ground motion was generated by a large rotating mass-shaking machine which was embedded in the ground at a distance of 12 m from the test wall. In addition, a small vibration exciter was mounted on the top of the wall in order to produce rocking. The displacements were measured at the top and bottom.

Figs. 7(a) and 7(b) show typical results of earth pressures and phase angles with varying frequencies observed during the ground motion test. The phase angles are referred to those of the displacement at the bottom. In this test, the amplitude of displacement at the bottom was of order of 0.3 mm at the frequency about 6 Hz. These measured results will be compared to the theory of horizontal translation, because the rocking mode was observed very little. The theoretical distribution given by Eq. (26) can be rewritten as

$$-\sigma_x|_{x=0} = \frac{GU_0}{H} \sqrt{S_1^2 + S_2^2}\, e^{i(\omega t + \theta_s)} \tag{36}$$

Thus, the dimensionless pressure $\sqrt{S_1^2 + S_2^2}$ and phase angle θ_s are plotted in Figs. 8(a) and 8(b), From comparison, a common feature will be recognized that the magnitude of pressure increases with depth, while the phase angle produces much more with approach to the free surface.

For the case of rocking, the similar comparison was examined. The experimental results of earth pressure and phase angle are shown in Figs. 9(a) and 9(b). On the other hand, the theoretical solution obtained in Eq. (34) can be rewritten as

$$\sigma_x|_{x=0} = G\Theta\sqrt{R_1^2 + R_2^2}\, e^{i(\omega t+\theta_R)} \tag{37}$$

where $\sqrt{R_1^2 + R_2^2}$ and θ_R are shown in Figs. 10(a) and 10(b). Again, both results appear to agree as a trend. In the quantitative comparison, the theoretical and observed earth pressures could be roughly coincided each other, if the shear modulus of sand is assumed as $G = 100\ kg/cm^2$. In this test, the amplitude of displacement at the top was of order of 0.44 mm at the frequency about 8.3 Hz.

CONCLUSION

The present paper demonstrated a theoretical analysis of dynamic earth pressures on a basement wall, when it undergoes horizontal translation and rocking. The validity of it was examined by experiments which was preformed on a retaining wall of gravity type. It is believed that the results obtained here will be useful to develope an equivalent mass-spring-dashpot system representing embedded structures.

ACKNOWLEDGEMENT

I wish to thank Mr. T. Hayashida and Mr. T. Imazawa who were responsible for much of the computer works.

REFERENCES

(1) H. Tajimi, "Dynamic Analysis of a Structure Embedded in an Elastic Stratum", Proc. 4th WCEE (Chile), 1969

(2) F. E. Richart, Jr., J. R. Hall, Jr. and R. D. Woods, "Vibrations of Soils and Foundations", Prentice-Hall Inc., p. 80

(3) W. D. Liam Finn, "Boundary Value Problems of Soil Mechanics", Proc. ASCE, SM 5, Sept. 1963

(4) Shin Niwa, "An Experimental Study of Oscillating Earth Pressure Acting on a Gravity Wall", Report of Ship Research Institute, Vol. 8, No. 5, Sept. 1971 (in Japanese)

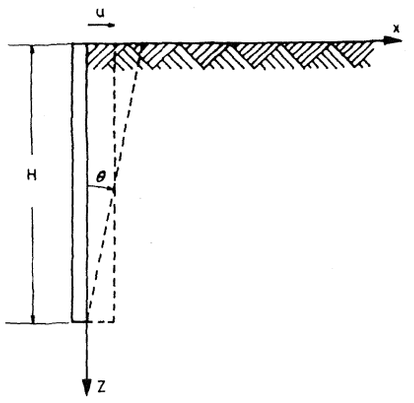

Fig. 1 Mathematical model

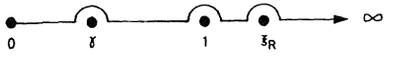

Fig. 2 Contour of integration

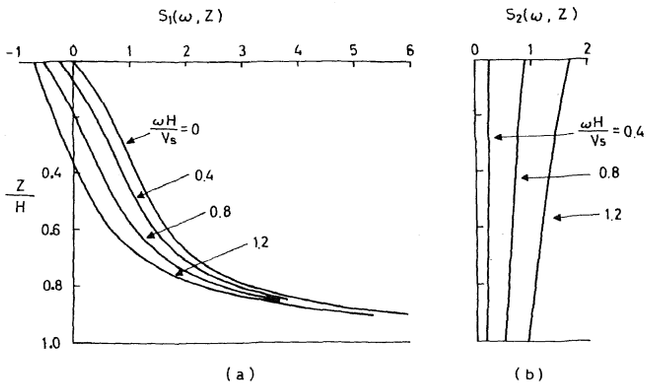

Fig. 3 Plots of $S_1(\omega, z)$ and $S_2(\omega, z)$ in Eq. (26) against z/H with variation of $\omega H/V_s$ for the case of $V_s/V_p = 1/3$

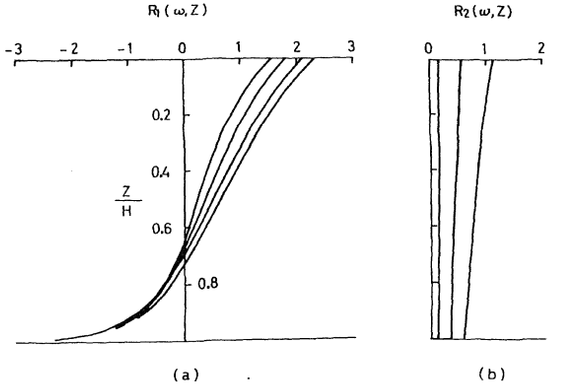

Fig. 5 Plots of $R_1(\omega, z)$ and $R_2(\omega, z)$ in Eq. (34) against z/H with variation of $\omega H/V_s$ for the case of $V_s/V_p = 1/3$

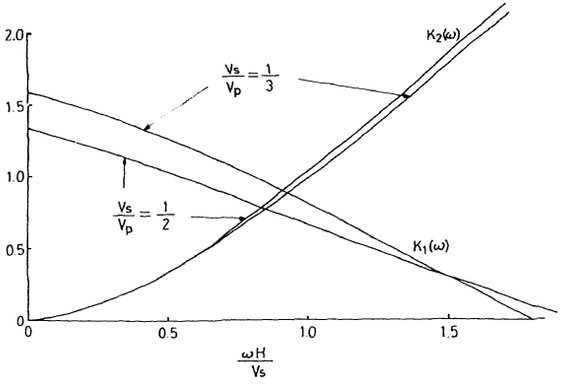

Fig. 4 Plots of $K_1(\omega)$ and $K_2(\omega)$ in Eq. (27) against $\omega H/V_s$ for the case of $V_s/V_p = 1/3$ and $1/2$

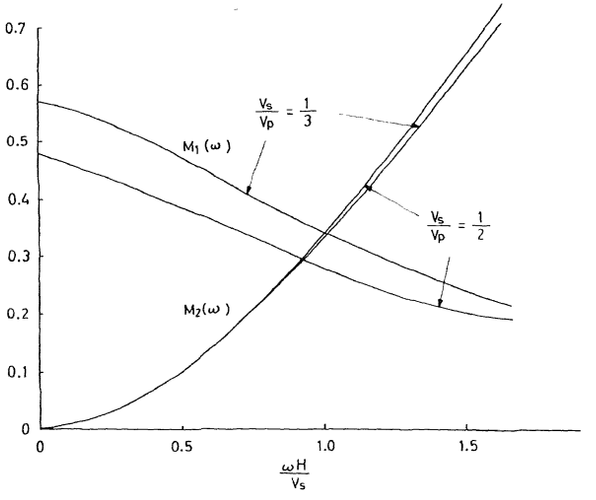

Fig. 6 Plots of $M_1(\omega)$ and $M_2(\omega)$ in Eq. (35) against $\omega H/V_s$ for the case of $V_s/V_p = 1/3$ and $1/2$

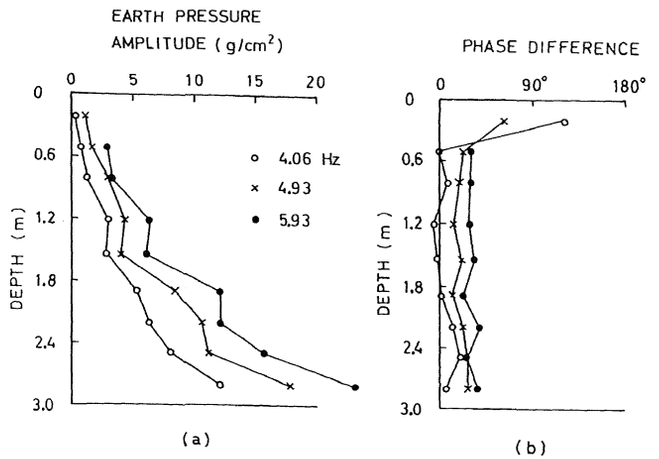

Fig. 7 Experimental distribution of earth pressure amplitude and phase difference, sway

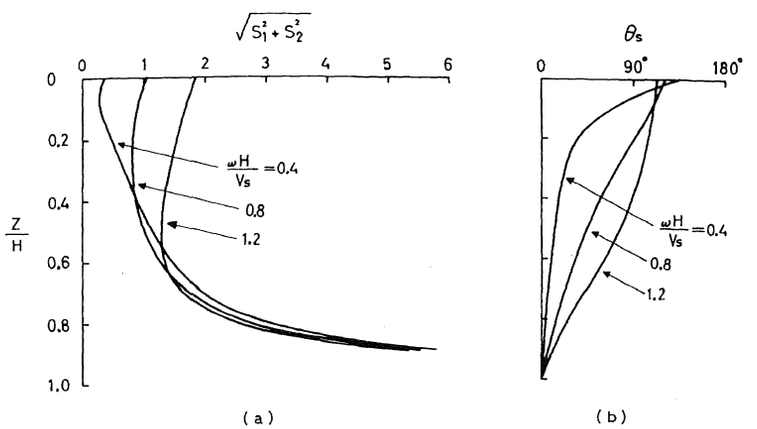

Fig. 8 Theoretical distribution of earth pressure amplitude and phase angle, horizontal translation, $V_s/V_p = 1/3$

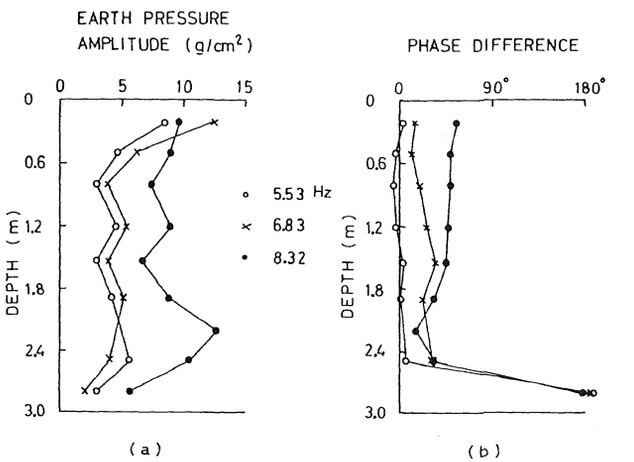

Fig. 9 Experimental distribution of earth pressure amplitude and phase difference, rocking

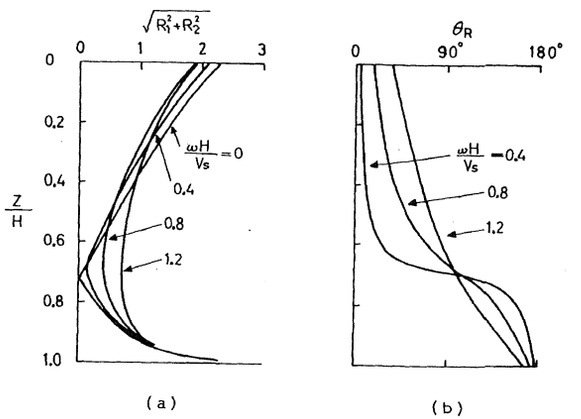

Fig. 10 Theoretical distribution of earth pressure amplitude and phase angle, rocking motion, $V_s/V_p = 1/3$